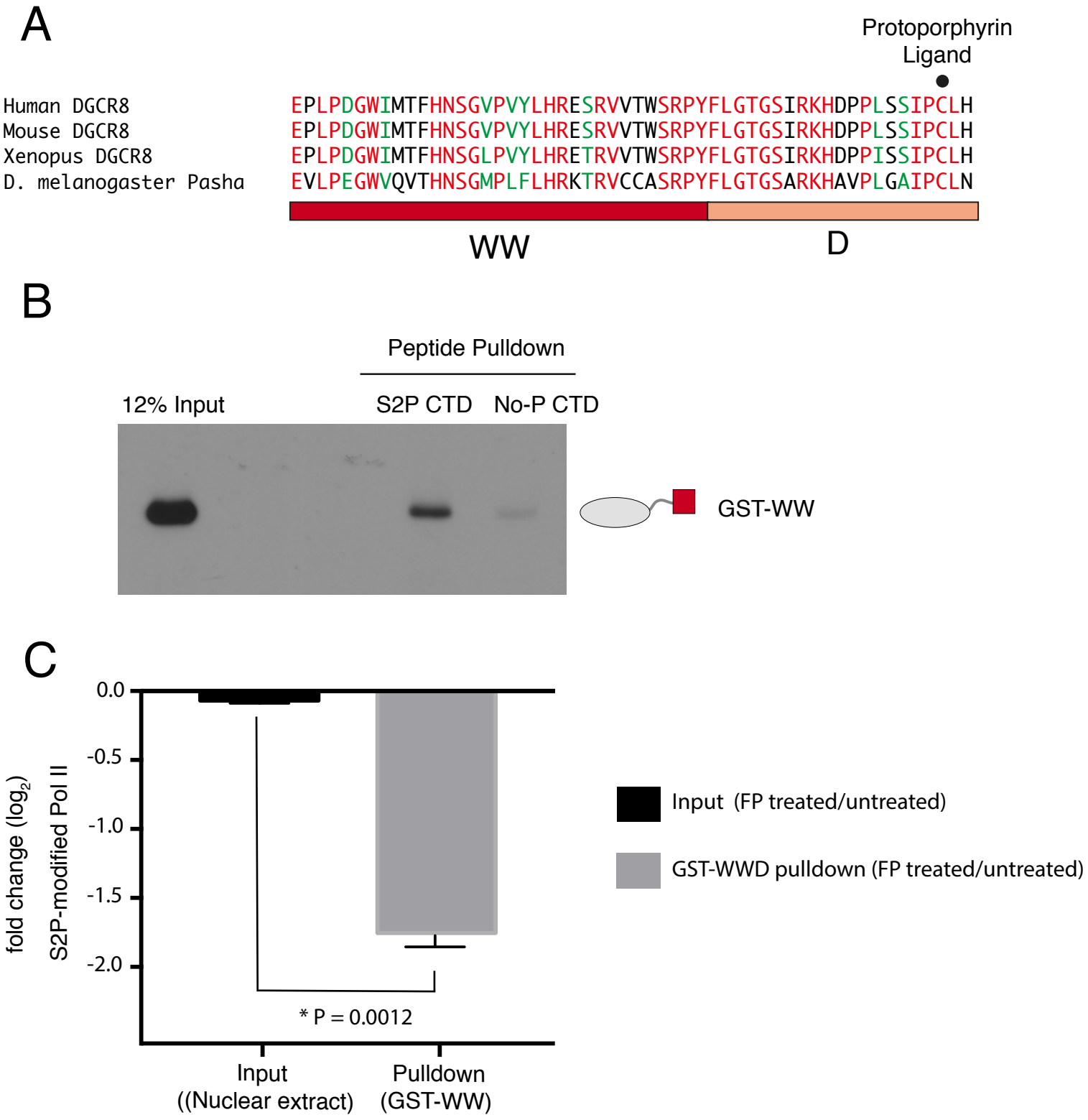

Figure S1. Structure-function of the WW domain. Related to Figsures 1, 2 and 3. (A) Amino-acid sequence alignment of the WW domain and carboxy-flank of DGCR8 homologs. Perfectly conserved residues are in red and residues with conservative amino acid differences are in green. The sequences used to create GST-WW and GST-WWD proteins are shown. GST-WWD includes a highly conserved region C-terminal to the WW domain that contains the heme-binding protoporphyrin cysteine residue involved in dimerization. (B) Binding between GST-WW protein and biotinylated peptides containing four CTD heptad repeats. Binding reactions were performed in high-stringency potassium phosphate buffer as described in Supplemental Experimental Procedures. Peptide-associated GST-WW protein was visualized by Western blot. Input shown represents 12% of total binding reactions. (C) Quantitation of change in S2P-modified Pol II that was pulled down by GST-WWD protein in nuclear extracts prepared from cells that had been treated for 2 hours with flavopiridol. Error bars are standard deviations and p-value is from a two-tailed t-test. Although the short treatment caused a slight reduction in total S2P-modified Pol II, it greatly reduced the S2P-modified Pol II that was free to bind to the GST-WWD bait.

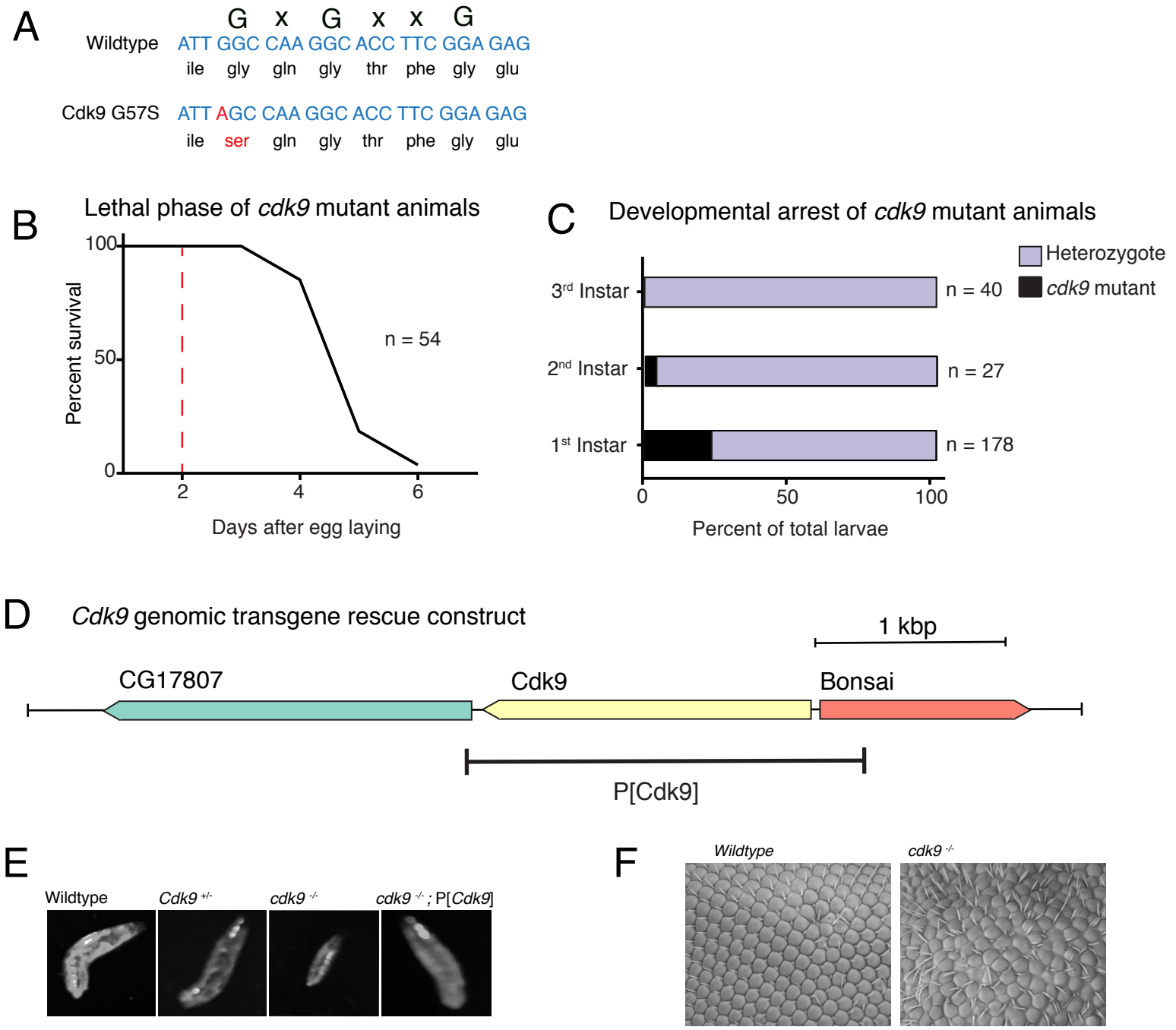

Figure S2. Molecular genetics of *cdk9*^{G57S} mutant and its *Cdk9* genomic rescue. Related to Figure 4
(A) Schematic showing the ATP-binding motif in the kinase domain of Cdk9. Sequencing of homozygous *cdk9* mutant larvae revealed a point mutation (red) resulting in a serine substitution at an invariant glycine residue. (B) Lethal phase analysis of *cdk9* mutant animals. Homozygous mutant animals die between 3 and 6 days after egg laying. Red dashed line marks the L1-L2 molt when we harvested mutant animals for all RNA and protein analysis. (C) Offspring from *cdk9* heterozygous balancer parents were scored for their *cdk9* genotype (heterozygous or homozygous) at different larval instar stages. If homozygous *cdk9* offspring developed normally, they should have represented 33% of the population at all stages. However, mutant representation was greatly diminished by the second and third instar stages. (D) Schematic of the genomic DNA used to create a rescue transgene for *cdk9*. (E) Wildtype, *cdk9* heterozygous, *cdk9* homozygous and rescued larvae at 72 hours after egg laying, when larvae are normally third instar. (F) Mitotic recombination was used to generate homozygous *cdk9* mutant eye cells in an otherwise heterozygous animal. Note the mispatterned eye facets suggesting a role for *cdk9* in eye development. However, the mutant is not cell-lethal since if it had been, no eye would have formed.

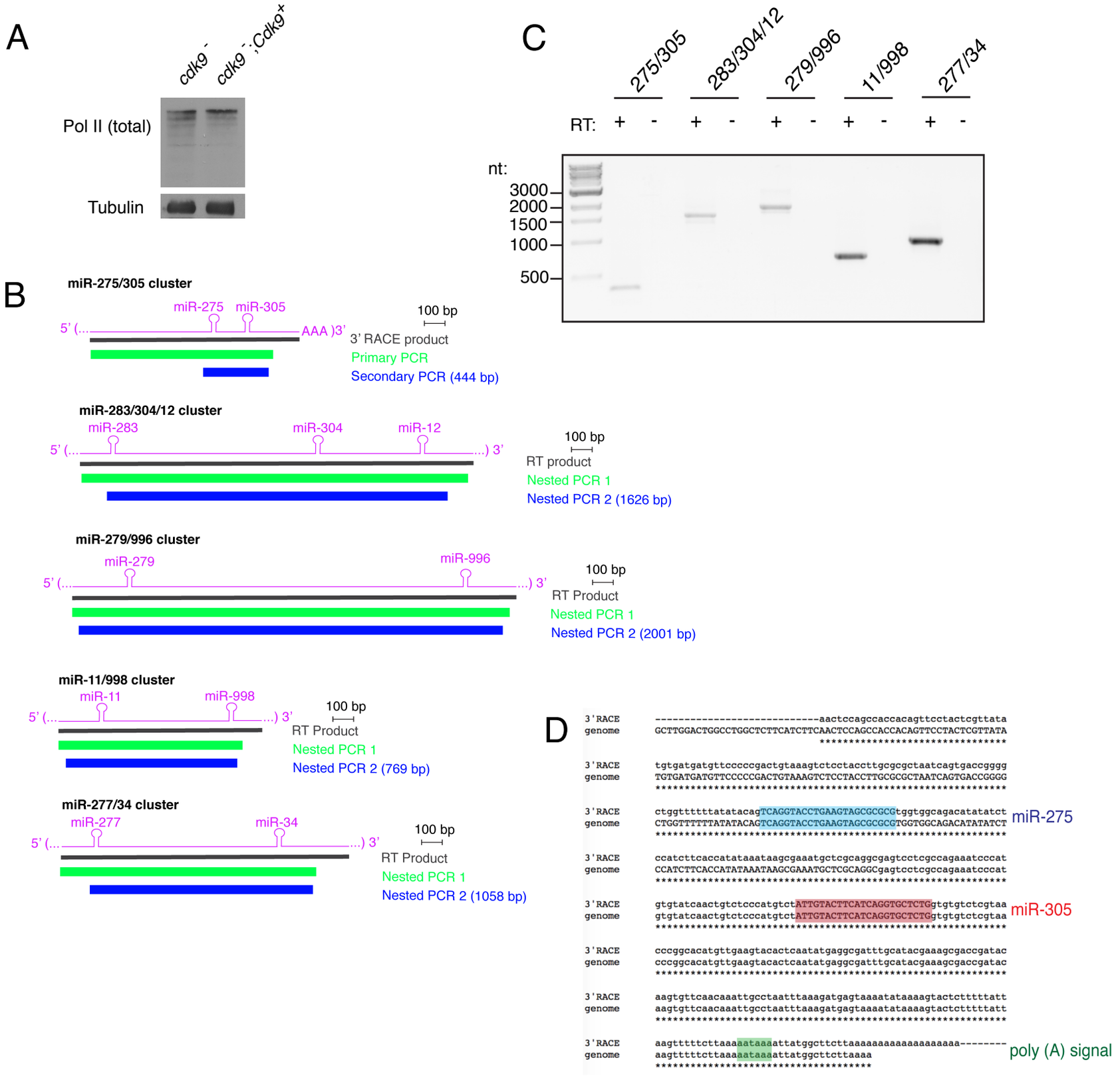

Figure S3. Analysis of polycistronic pri-miRNAs affected by *cdk9*. Related to Figure 5. (A) Western blot of total Pol II using antibody 4H8 from *cdk9* mutant and rescued larvae. (B) Schematics of the five polycistronic transcripts showing the relevant regions analyzed by nested RT-PCR. Black, green and blue lines correspond to predicted cDNAs, primary amplicons, and secondary amplicons, respectively. Sizes of predicted secondary amplicons are shown. Note the secondary amplicons span all pre-miRNAs for a given pri-miRNA. (C) Stained agarose gel with nested PCR reaction products, as indicated. Each product is the predicted size for secondary amplicons as in B. (D) Alignment of the sequenced 3'RACE product generated from pri-miR-275/305 RNA with release 6 of the *Drosophila* genome. Primary features are highlighted.

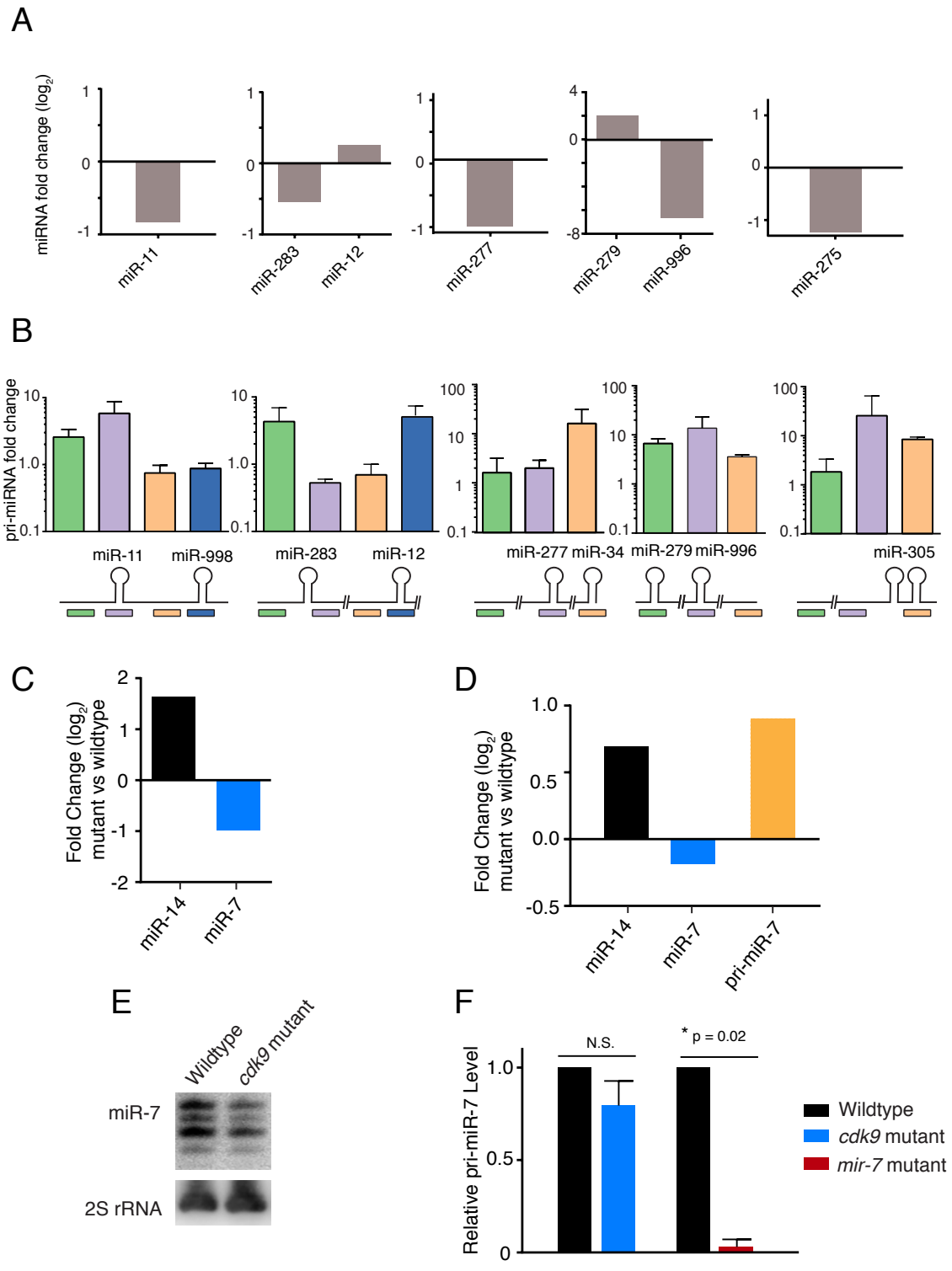

Figure S4. Analysis of miRNAs dependent on *cdk9*. Related to Figure 5. (A) Fold change (log2) of mature miRNA levels as measured by splinted-ligation assays in *cdk9* mutant relative to wildtype. Some of the mature miRNAs were below the level of detection by the assay and are not included. (B) Differential expression of pri-miRNAs between *drosha* mutant and wildtype larvae, as determined by RT-qPCR. Shown below each plot are positions of the various RT-qPCR products being assayed. Error bars are standard deviations. (C) Fold change (log2) of miR-14 and miR-7 sequencing reads in *cdk9* mutant relative to wildtype libraries. (D) Northern analysis of miR-14 and miR-7 RNAs extracted from *cdk9* mutant and wildtype larvae. For miR-7, it was possible to detect the pri-miRNA species as well. RNAs were normalized to 2S rRNA, and fold change (log2) in *cdk9* mutant relative to wildtype is shown. (E) Northern blot of mature miR-7 extracted from adult heads. These heads were genotypic chimeras, with all eye cells being *cdk9* mutant. The wildtype samples had a copy of the *Cdk9* rescue transgene. (F) RT-qPCR of pri-miR-7 from adult heads with *cdk9* mutant eyes. No significant difference in pri-miR-7 was detected in *cdk9* mutants compared to wildtype. Head RNA from *mir-7* null mutants was also analyzed to test the specificity of pri-miR-7 primers.

A

GMR>GFP::Brd CDS and 3'UTR

AUGGUGAGCAAGGGCGAGGAGCUGUUCACCGGGGUGGUGCCCAUCCUGGU
CGAGCUGGACGGCGACGUAAACGGCCACAAGUUCAGCGUGUCCGGCGAGG
GCGAGGGCGAUGCCACCUACGGCAAGCUGACCCUGAAGUUCAUCUGCACC
ACCGGCAAGCUGCCCGUGCCCUGGCCCACCCUCGUGACCACCCUGACCUA
CGGCGUGCAGUGCUUCAGCCGCUACCCCGACCACAUGAAGCAGCACGACU
UCUUCAAGUCCGCCAUGCCCGAAGGCUACGUCCAGGAGCGCACCAUCUUC
UUCAAGGACGACGGCAACUACAAGACCCGCGCCGAGGUGAAGUUCGAGGG
CGACACCCUGGUGAACCGCAUCGAGCUGAAGGGCAUCGACUUCAAGGAGG
ACGGCAACAUCCUGGGGCACAAGCUGGAGUACACUACAACAGCCACAACG
UCUAUAUCAUGGCCGACAAGCAGAAGAACGGCAUCAAGGUGAACUUCAAG
AUCCGCCACAACAUCGAGGACGGCAGCGUGCAGCUCGCCGACCACUACCA
GCAGAACACCCCCAUCGGCGACGGCCCCGUGCUGCUGCCCGACAACCACU
ACCUGAGCACCCAGUCCGCCCUGAGCAAAGACCCCAACGAGAAGCGCGAU
CACAUGGUCCUGCUGGAGUUCGUGACCGCCGCCGGGAUCACUCUCGGCAU
GGACGAGCUGUACAAGUAAAGCGGCCGCAAAAGCUGGUACCUCGAGGAAA
AUGGGAAAUCCGAAAAAAAAUACCACUUUCCAAUCAGCUUUAAAGACUCC
AACGGAUUCGGUCUCUAAACAUCAUCCGCAACAGCUUUAACUCUCCACAC
UGUGCAAGUGGAGAUUUUAAAAUGAAAUGCACAAAUAUCCAGCUUUAAUC
AUUGUCUUCCAUCUAUGUUUAAGAGAGUAUGAAUAAAUACAUAAUAUUAA
UACCGAAACUUGUUUGCAUUUCUGAUUUCUUAUUCGAACUUUCCCUUUGU
CAUUGUAAUUUCCUCGAAGGUUUUUCCAAGAAUCUGUAAGCCAAAAACCG
UUCUUAUCCCGUACCCCUGACCCUUCCACAUUCACGGAA

B

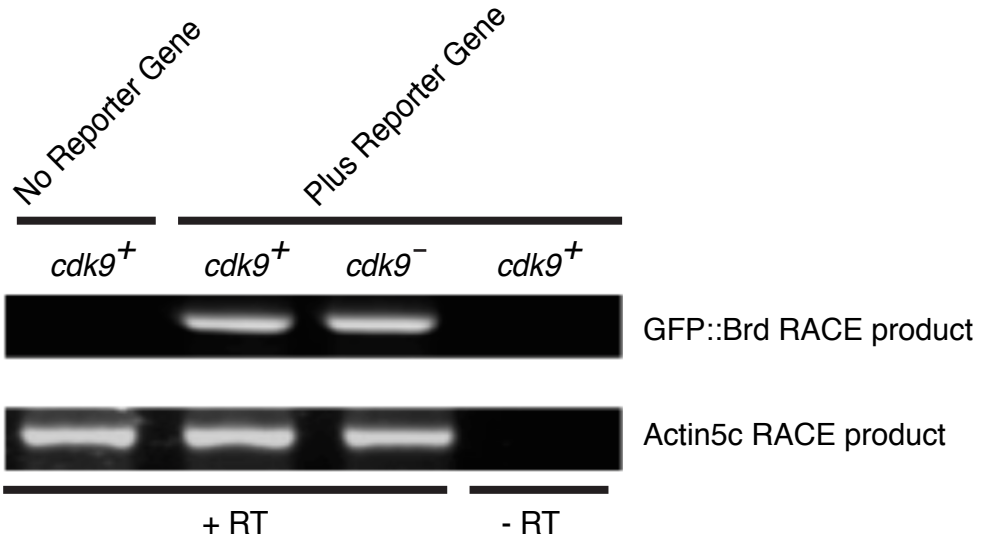

Figure S5. Analysis of Brd reporter expression. Related to Figure 6. (A) Schematic of the Brd reporter transgene that is expressed from the eye-specific GMR promoter. Green sequence is the GFP open reading frame and red sequence is the stop codon. Location of the forward cDNA primer used in 3'RACE analysis is underlined. Boxed is the M8-A1 8mer seed match to miR-7 in the Brd 3'UTR. Expression of the Brd reporter is dependent on miR-7, as determined by loss-of-function and gain-of-function experiments (data not shown). (B) Brd reporter mRNA 3'RACE products generated from total RNA from adult heads. Stained agarose gel with reaction products, as indicated. Each product is the predicted size for an amplicon as predicted in A. Moreover, no difference was detected in 3'-end structure after sequencing the 3'-RACE products derived from cdk9 mutant and wildtype tissue (data not shown).

Table S1. Small RNA-Seq Data. Related to Figure 5.

	Wildtype Reads	Cdk9 Mutant Reads	DESEQ2 normalization by library size	Wildtype Normalized	Cdk9 Mutant Normalized
MI0000128_2	74959	361293	MI0000128_2	826732.1142	327548.5845
MI0000136_2	109726	351685	MI0000136_2	121016.7142	318837.9624
MI0000116_2	92686	311818	MI0000116_2	102223.3124	282694.5015
MI0000129_1	226832	128732	MI0000129_1	250172.8243	116708.5562
MI0000130_1	69194	68302	MI0000130_1	76314.0051	61922.6595
MI0000135_2	67925	40964	MI0000135_2	74914.42605	37138.00217
MI0000134_1	67924	40961	MI0000134_1	74913.32315	37135.28236
MI0000387_2	25946	63019	MI0000387_2	28615.82184	57133.08657
MI0000131_1	48758	23289	MI0000131_1	53775.15768	21113.83001
MI0000126_1	28414	37551	MI0000126_1	31337.77699	34043.77305
MI0000124_1	28073	37341	MI0000124_1	30961.68837	33853.38685
MI0000125_1	28042	37278	MI0000125_1	30927.4985	33796.27099
MI0005857_2	32246	25767	MI0005857_2	35564.0866	23360.38721
MI0000412_1	21127	36515	MI0000412_1	23300.95074	33104.53445
MI0000130_2	11610	43558	MI0000130_2	12804.65935	39489.72508
MI0005813_2	37132	14336	MI0005813_2	40952.85194	12997.03152
MI0005812_1	21789	27877	MI0005812_1	24031.06999	25273.31526
MI0000373_2	15666	33226	MI0000373_2	17278.01838	30122.72385
MI0000359_2	12389	36114	MI0000359_2	13663.8178	32740.98746
MI0000368_1	34187	12861	MI0000368_1	37704.81389	11659.79508
MI0000360_2	32836	12825	MI0000360_2	36214.79711	11627.15745
MI0000127_1	27307	14140	MI0000127_1	30116.86761	12819.33773
MI0000363_2	11789	26764	MI0000363_2	13002.0783	24264.26838
MI0000354_1	7821	25956	MI0000354_1	8625.774401	23531.7348
MI0000420_2	6665	25048	MI0000420_2	7350.822961	22708.54111
MI0000415_1	19080	11718	MI0000415_1	21043.31614	10623.55018
MI0000117_1	5289	24679	MI0000117_1	5833.233705	22374.00536
MI0000118_1	5247	24648	MI0000118_1	5786.91194	22345.90073
MI0000128_1	15442	9544	MI0000128_1	17030.96897	8652.599665
MI0005862_2	14217	10208	MI0005862_2	15679.91749	9254.582709
MI0000118_2	14686	8039	MI0000118_2	16197.1772	7288.165204
MI0000414_1	12041	10226	MI0000414_1	13280.00889	9270.901527
MI0000356_2	18435	2993	MI0000356_2	20331.94618	2713.456705
MI0000426_2	14032	5199	MI0000426_2	15475.88114	4713.418447
MI0000123_1	8244	10029	MI0000123_1	9092.300749	9092.301135
MI0005808_1	1089	17118	MI0005808_1	1201.057195	15519.19542
MI0000123_2	6006	12088	MI0000123_2	6624.012409	10958.99253
MI0000428_2	6397	9598	MI0000428_2	7055.245984	8701.556117

MI0005861_1	8987	6360	MI0005861_1	9911.754832	5765.982174
MI0000413_1	8781	5750	MI0000413_1	9684.557603	5212.955582
MI0000419_1	7552	6370	MI0000419_1	8329.094524	5775.048184
MI0000129_2	10272	3016	MI0000129_2	11328.98026	2734.308528
MI0000364_1	5536	7707	MI0000364_1	6105.6498	6987.173681
MI0005858_2	9245	3214	MI0005858_2	10196.30282	2913.81552
MI0005812_2	9381	2992	MI0005812_2	10346.2971	2712.550104
MI0000427_1	5522	6754	MI0000427_1	6090.209211	6123.182956
MI0000119_1	3279	8807	MI0000119_1	3616.406375	7984.434749
MI0000120_1	3115	8736	MI0000120_1	3435.530911	7920.06608
MI0000387_1	6750	4904	MI0000387_1	7444.569391	4445.97116
MI0000132_1	2800	8696	MI0000132_1	3088.117673	7883.802042
MI0000382_1	1009	10029	MI0000382_1	1112.825262	9092.301135
MI0000370_2	6575	4056	MI0000370_2	7251.562036	3677.173537
MI0000432_1	504	10094	MI0000432_1	555.8611812	9151.230199
MI0005856_2	5059	4702	MI0005856_2	5579.566896	4262.837764
MI0005838_1	4716	4758	MI0005838_1	5201.272481	4313.607419
MI0005845_1	5143	4253	MI0005845_1	5672.210426	3855.773929
MI0000133_1	2346	5830	MI0000133_1	2587.40145	5285.483659
MI0005827_2	3484	4661	MI0005827_2	3842.500705	4225.667125
MI0000410_2	1113	6911	MI0000410_2	1227.526775	6265.519309
MI0005871_2	3821	3360	MI0005871_2	4214.177725	3046.179262
MI0000374_2	4135	2835	MI0000374_2	4560.488064	2570.213752
MI0005864_2	2354	4422	MI0005864_2	2596.224644	4008.989493
MI0005820_1	3367	2885	MI0005820_1	3713.461502	2615.543801
MI0005846_2	2766	3284	MI0005846_2	3050.619101	2977.277588
MI0000366_1	2406	3424	MI0000366_1	2653.575401	3104.201724
MI0000370_1	2406	3424	MI0000370_1	2653.575401	3104.201724
MI0000357_2	2468	3237	MI0000357_2	2721.955149	2934.667342
MI0005821_1	1404	4103	MI0005821_1	1548.470433	3719.783783
MI0005847_1	410	4973	MI0005847_1	452.1886593	4508.526627
MI0000120_2	3576	1569	MI0000120_2	3943.967428	1422.456923
MI0000380_1	2215	2924	MI0000380_1	2442.921659	2650.901238
MI0000135_1	2584	2303	MI0000135_1	2849.891453	2087.902036
MI0000122_1	1811	2843	MI0000122_1	1997.350395	2577.46656
MI0005867_1	2772	1543	MI0005867_1	3057.236496	1398.885298
MI0000367_1	2494	1630	MI0000367_1	2750.630527	1477.759582
MI0000411_1	2342	1762	MI0000411_1	2582.989854	1597.43091
MI0005849_1	570	3056	MI0005849_1	628.6525263	2770.572567
MI0000379_2	1405	2185	MI0000379_2	1549.573332	1980.923121
MI0000361_2	1056	2532	MI0000361_2	1164.661522	2295.513658

MI0000369_2	2406	1037	MI0000369_2	2653.575401	940.1452067
MI0000429_2	693	2727	MI0000429_2	764.3091241	2472.300847
MI0005860_1	1132	2157	MI0005860_1	1248.481859	1955.538294
MI0000412_2	637	2523	MI0000412_2	702.5467706	2287.354249
MI0000362_2	1347	1512	MI0000362_2	1485.605181	1370.780668
MI0005810_1	1073	1699	MI0005810_1	1183.410808	1540.315049
MI0005873_1	1125	1637	MI0005873_1	1240.761565	1484.105789
MI0000136_1	1991	407	MI0000136_1	2195.872245	368.9865951
MI0000356_1	1862	429	MI0000356_1	2053.598253	388.9318164
MI0000371_1	1234	1020	MI0000371_1	1360.977575	924.7329901
MI0000383_2	1194	716	MI0000383_2	1316.861608	649.126295
MI0005811_1	872	859	MI0005811_1	961.7280754	778.7702339
MI0000431_1	374	1314	MI0000431_1	412.4842892	1191.273676
MI0000418_1	384	1290	MI0000418_1	423.5132809	1169.515252
MI0000420_1	961	692	MI0000420_1	1059.886101	627.3678717
MI0005870_1	679	797	MI0005870_1	748.8685357	722.5609737
MI0000410_1	558	814	MI0000410_1	615.4177363	737.9731902
MI0000116_1	472	847	MI0000116_1	520.5684078	767.8910222
MI0005869_1	1173	134	MI0005869_1	1293.700725	121.4845301
MI0005847_2	977	236	MI0005847_2	1077.532488	213.9578291
MI0000375_2	251	879	MI0000375_2	276.8276914	796.9022533
MI0000374_1	846	177	MI0000374_1	933.052697	160.4683718

Table S2. Drosophila Strains. Related to Figures S2 - S5 and 6.

Brd reporter assay:

Fig. 6A) *y w, ey-FLP; FRT42D, Cdk9^{G57S} / FRT42D, GMR>myr-RFP; GMR > GFP::Brd*

Fig. 6B) *y w, ey-FLP; FRT42D, Cdk9^{G57S}/ FRT42D, GMR>myr-RFP; GMR > GFP::Brd / P[Cdk9]*

Apoptosis Assay:

Fig. 6C) *rbf1^{120a}, eyFLP; act5c>CD2>GAL4, UAS-GFP*

Fig. 6D*) rbf1^{120a}, eyFLP; act5c>CD2>GAL4, UAS-mir-998*

Fig. 6E) *rbf1^{120a}, eyFLP; FRT42D, Ubi>GFP / FRT42D, Cdk9^{G57S}*

Other Assays:

y w, ey-FLP; FRT42D, Cdk9^{G57S}

y w, ey-FLP; FRT42D

y w, ey-FLP; FRT 42D, Cdk9^{G57S} / FRT42D, GMR>Hid, cl

y w, ey-FLP; FRT 42D, Cdk9^{G57S} / FRT42D, GMR>Hid, cl ; P[Cdk9]

miR-7$^{\Delta 1}$ / Df(2R)exu1

Table S3. Oligonucleotides used in the study. Related to Figure 4.

qPCR primers	
Pri-miR-11/998_1F	CGATGCTCTCTTCAACGACA
Pri-miR-11/998_1R	GTTACAGGCGGATGCAAAAT
Pri-miR-11/998_2F	AGGCGCACTTGTCAAGAACT
Pri-miR-11/998_2R	GTTGGCCGAAAGGTTGTAAA
Pri-miR-11/998_3F	AGTAAACCACCCAACCGACA
Pri-miR-11/998_3R	TGAATTTGACACGAGGACGA
Pri-miR-11/998_4F	CTCCAGGGCAAATTGTTCAT
Pri-miR-11/998_4R	GGCTGGCTGCATATGATTTT
Pri-miR-283/304/12_F1	CCCGCGATTCACTTGACTAA
Pri-miR-283/304/12_R1	TCTCTCTCTCGCTCCCAAAG
Pri-miR-283/304/12_F2	TCACCATAAGCGCAACAAAA
Pri-miR-283/304/12_R2	ACCTGTGAGGTGAGGTGAGC
Pri-miR-283/304/12_F3	TTGTTGTTGATCGCTGCTTC
Pri-miR-283/304/12_R3	AACGGATGGTACGGTTTACG
12 flankF1	GACGCACTGAAGGATCGTCT
12 flankR1	TGATCATGTGAGTGGAACTCG
Pri277/34_F1	GCGCCTGCCACTTATTACAT
Pri277/34_R1	GGCCGAAAAGACATCGATAA
277_flankF1	AACGAGGCCTAACGATAAAATG
277_flankR1	TTATCGCATTTTCCTGCATTC
34_flankF1	TAATTGGCTATGCGCTTTGG
34_flankR1	TGCCATAACCATCTGATACAGG
Pri275/305_F1	GCGACGGAGACCTAATACCA
Pri275/305_R1	ATGGCAACAAAACTGCATCA
Pri275/305_F2	TCGTGTGTGAGAAGCAAAGC
Pri275/305_R2	CTGTCGCTCGAATTTCACAA
Pri275/305_F3	GAAATGCTCGCAGGCGAGTCC
Pri275/305_R3	GTTGAACACTTGTATCGGTCGC
Pri-miR-7_F	CTGCTTCTGCTCCTGTTCCT
Pri-miR-7_R	GGGAGTGTCCCGTGTAAGTG
Pri-miR-279/996_F1	TTGAAATTAAAGAGGAGGCGAG
Pri-miR-279/996_R1	AAGTTTGTCAAGAAAACACGTGC
Pri-miR-279/996_F2	GTCACTCAGTCCGTCCCAAT
Pri-miR-279/996_R2	AACCAAGAAGCCAAAGACGA
996 flankF1	CCAATCACAAAAATGCCACA
996 flankR1	CGTTGTGCTGACCCAACTTA
RPL32 F	GACGCTTCAAGGGACAGTATCTG
RPL32 R	AAACGCGGTTCTGCATGAG

3'RACE and Nested PCR primers	
998,11 R0	AATGTTCTGCAGTTCGGGG
998,11 Outer F	CAACCGATCATGCCTGCAAC
998,11 Outer R	AGAGCGAGAGATGTTGTGGA
998,11 Inner F	ATTTTGCATCCGCCTGTAAC
998,11 Inner R	ACGCCAGAGCTGAATCTCAT
283,12,34 R0	GGCATGAGAAAAGGAGCAAA
283,12,34 Outer F	TGGGAGCGAGAGAGAGAGAG
283,12,34 Outer R	TGAAAGTTGAATGGGCGTTT
283,12,34 Inner F	TGTCACCTCACACGATTCTCA
283,12,34 Inner R	TGTTGGTCATGCGGTTAGTG
279,996 R0	GGCGCTTGCTACGAGTATCT
279,996 Outer F	GCCGCTTATCAACGCTAAAA
279,996 Outer R	TTTTTCGGTAGTTGCTGCTG
279,996 Inner F	AAAAAGAAGGAGGAACAGAAACG
279,996 Inner R	CACTCGATGTGGGTCACG
277,34 R0	GGTTGAGCAGTTGCCAAACTA
277,34 Outer F	ATCGATAGACTGCCCCACAG
277,34 Outer R	TTCCAGACAATCCGATGTGA
277,34 Inner F	GCATCCTTTGAAGGTTTTGG
277,34 Inner R	CCTCCGCCATGTCCTTTAT
275/305_GSP1	AACGAAACGCAAGGAAAAG
275/305_GSP2	AACTCCAGCCACCACAGTTC
Brd 3'RACE GSP1	CGACAACCACTACCTGAGCACC
Brd 3'RACE GSP2	GAGAAGCGCGATCACATGGTCC
Q_T	CCAGTGAGCAGAGTGACGAGGACTCGAGCTCAAGCTTTTTTTTTTTTTTTT
Q_o	CCAGTGAGCAGAGTGACG
Q_I	GAGGACTCGAGCTCAAGC

Cloning Primers	
Pasha_Entry_F	GGCCGCCGTACTCGAGGCGGAGAAGCCGCTGGCCGACT
Pasha_Entry_R	CTGGGTCGGCGCGCCGCGCTCAAAGTTCCACGTTGTTCAA
GFP-Pasha_pmk33_F	TATTATCTCGAGGCCACCATGGTGAGCAAGGGCGAGGAGCT
GFP-Pasha_pmk33_R	GCGGCGGGATCCTCAAAGTTCCACGTTGTTCAA
GST-Pasha_pGEX_F	GGTTCCGCGTGGATCCATATTAGCGGAGAAGCCGCTGGCCGACT
GST-Pasha_pGEX_R	ATGCGGCCGCTCGAGCGCTCAAAGTTCCACGTTGTTCAA
WW_ pGEX_F	GCGGATCCATTATGTTCAAGACTGTGCTGGAAGAA
WW_ pGEX_R	GCCTCGAGCTCCAAAGCCCGCCTGTAGTT
WWD_ pGEX_F	GCGGATCCATTATGCGCCTCAACCACTTTGAAGTC
WWD_ pGEX_R	GCCTCGAGACTTCCAGTGCCGAGAAAATA

Splinted Ligation Oligos	
ligation oligo	5′-CGCTTATGACATTC/dideoxyc/-3′
bridge_ mir-11	5’-GAATGTCATAAGCGGCAAGAACTCAGACTGTGATG /3spc3/-3’
bridge_mir-283	5’-GAATGTCATAAGCGCCAGAATTACCAGCTGATATTT /3spc3/-3’
bridge_mir-12	5’-GAATGTCATAAGCGACCAGTACCTGATGTAATACTCA /3spc3/-3’
bridge_mir-277	5’-GAATGTCATAAGCGTGTCGTACCAGATAGTGCATTTA /3spc3/-3’
bridge_mir-279	5’-GAATGTCATAAGCGTTAATGAGTGTGGATCTAGTCA /3spc3/-3’
bridge_mir-996	5’-GAATGTCATAAGCGAGACGAGCATGAAATCTAGTCA /3spc3/-3’
bridge_mir-275	5’-GAATGTCATAAGCGCGCGCGCTACTTCAGGTACCTGA /3spc3/-3’
bridge_2S rRNA	5’-GAATGTCATAAGCGTACAACCCTCAACCATATGTAGTCC A/3spc3/-3’

Northern Blot Probes	
2S rRNA	TACAACCCTCAACCATATGTAGTCCAAGCA
dme-miR-7 LNA (Exiqon)	ACAACAAAATCACTAGTCTTCCA
dme-miR-14 LNA (Exiqon)	ATAGGAGAGAGAAAAAGACTGA

SUPPLEMENTAL EXPERIMENTAL PROCEDURES

Immunoprecipitations

To immunoprecipitate GFP-Pasha, cells were lysed in 10 mM Tris-Cl pH 7.5, 150 mM NaCl, 0.5 mM EDTA, 0.5% NP-40 with phosphatase inhibitors and protease inhibitors (10 mM NaF, 1 mM Na_3VO_4, 0.5 µg/mL MG132, 10 µg/mL soybean trypsin inhibitor, 3.6 µg/mL aprotinin, 2 µg/mL pepstatin A, 1 mM PMSF). Lysate was spun 15 minutes at 16,000xg at 4°C. Supernatant was adjusted to 1 mg/ml protein with wash buffer (lysis buffer without NP-40). One ml of extract was incubated overnight with 20 µL of washed GFP-Trap A beads (Nanotrap). The reaction was then spun at 2,500xg at 4°C and beads were washed once in lysis buffer and three times in wash buffer with phosphatase inhibitors before eluting with 2X SDS loading buffer.

To immunoprecipitate Pol II, cells were lysed in 50 mM HEPES-KOH pH 7.5, 150 mM KCl, 1.5 mM $MgCl_2$, 1.5 mM EGTA, 10% glycerol and 0.2% NP-40 with protease and phosphatase inhibitors. Lysates were spun for 15 minutes at 16,000xg and the supernatants were pre-cleared by 1 hour rotating at 4°C with 10 µL washed protein G IgG magnetic beads (Dynabeads). Immunoprecipitation reactions were performed overnight at 4°C with 0.5 ml of 1 mg/ml protein extract and 1 µg antibody, either Abcam ab5095 (Ser2P), ab5131 (Ser5P), ab5408 (Ser5P), 8W16G (hypophosphorylated Pol II), or 4H8, which recognizes all CTD isoforms of Pol II (Brodsky et al., 2005; Schroder et al., 2013). Reactions were centrifuged at 10,000xg, 10 minutes at 4°C and the supernatants were incubated with 10 µL protein G IgG magnetic beads for 2 hours at 4°C. Beads were washed four times in 50 mM HEPES-KOH pH 7.5, 150 mM KCl with phosphatase inhibitors and eluted with 2X SDS loading buffer.

Precipitate samples were subjected to 8 or 10% SDS-PAGE and wet-transferred to PVDF membrane. Membranes were blocked in 5% non-fat dry milk in TBS, 0.05% Tween-20 and incubated overnight at 4°C in primary antibody in blocking solution. Antibodies used were anti-Pol II antibodies at 1 µg/mL, 1:2000 anti-Pasha (gift of G. Hannon), anti-GFP at 0.5 µg/ml (GFP-Tag antibody, Molecular Probes) or anti-alpha-tubulin at 0.9 µg/ml (12G10, Developmental Studies Hybridoma Bank).

To determine if RNA was required for the interaction between Pol II and Pasha, 500 µg cell extract were incubated overnight with ab5408 as described above. Before incubation with protein G beads, samples were treated with 30 µg RNase A and 5000 U RNase T1 for 2 hours at 16°C. Control experiments determined that this treatment was sufficient to degrade bulk RNA in the extract (data not shown). Samples were then spun 10,000xg, 10 minutes at 4°C to remove precipitates and incubated with protein G IgG magnetic beads. The remaining steps were carried out as described above.

GST Protein Purification

To generate GST fusion proteins, bacteria were cultured in LB + 1% (w/v) glucose + 30 µg/ml hemin (Sigma), which is amenable for expressing heme-binding proteins such as human hemoglobin (Hoffman et al., 1990). IPTG was added to induce GST fusion protein expression, and GST proteins were purified using standard procedures (Sambrook and Russell, 2001). Purified proteins were stored in 25 mM HEPES pH 7.5, 100 mM NaCl, 2 mM EDTA, 1 mM DTT, 10% glycerol, with protease and phosphatase inhibitors.

Peptide Binding Assays

CTD peptides with four repeats of YSPTSPS and amino-terminal biotinylation were described previously (Kim et al., 2004), and were synthesized by the BCMP Biopolymers facility at Harvard Medical School. Peptides were either unmodified, or phosphorylated on serine-2, serine-5, or serine-2 and serine-5. 500 µg of streptavidin-coupled magnetic beads (M280 Dynabeads; Invitrogen) were incubated with 1 µg of biotinylated peptide for 60 min at 4°C in 500 µl of coupling buffer: 25 mM Tris-Cl (pH 7.6), 50 mM NaCl, 1 mM DTT, 5 % glycerol, 0.03 % Triton X-100, protease and phosphatase inhibitors. Beads were washed three times with 500 µl of ice-cold coupling buffer. Beads with 1 µg of coupled peptide were then mixed with 100 µl of GST fusion protein in 50 mM HEPES pH7.5, 20 mM NaCl, 50 mM KOAc, 10 mM Mg_2OAc, 1 mM EDTA, 1 mM DTT, 10% glycerol, 0.1% NP-40, 0.05% Triton X-100, protease and phosphatase inhibitors, and BSA such that total protein concentration was constant at 1 mg/ml. GST fusion protein was adjusted such that its concentration was 5.0 µM, and the GST/peptide molar stoichiometry was 2:1. Reactions were incubated overnight at 4°C with mixing. The beads were then washed 3 - 5 times in 0.5 ml ice-cold binding buffer before elution in SDS-PAGE loading buffer. To assay for high-stringency binding, beads with 1 µg of coupled peptide were mixed with 5.0 µM GST fusion protein in 10 mM Potassium Phosphate pH7.7, 100 mM KOAc, 20 mM Mg_2OAc, 5 mM EGTA, 10% glycerol, 0.1% NP-40, and 0.05% Triton X-100 (Kim et al., 2004). Incubation and washing was performed as above. For all reactions, input loaded on the SDS-PAGE gel was 0.1% of the total reaction, while bound eluate was 2% of the total reaction. The anti-GST Western blot was scanned and quantitated. Intensity of eluate GST-WWD band

was approximately five-fold greater than intensity of the input band. Thus, 25% of total GST-WWD protein formed a stable complex with peptide. If we assume a 1:1 binding stoichiometry between peptide and protein, then the K_d is approximately 3.75 μM.

GST Pulldown Assays

Nuclear lysates of S2 cells were prepared essentially as described (Wright et al., 2006). Approximately $1x10^8$ cells were washed and suspended in 2 packed-cell volumes of Buffer A. This was incubated on ice for 30 min. Triton X-100 was added to a final concentration of 0.1% (v/v). Cells were homogenized with a type B Dounce homogenizer until 80 - 90% lysis was achieved. Nuclei were pelleted at 7,650×g for 10 min in the cold, and resuspended in 4 pellet volumes of Buffer B. Nuclei were lysed by adding $1/10^{th}$ volume of 4 M $(NH4)_2SO_4$ and then gently mixed for 30 min at 4^oC to avoid shearing DNA. The lysate was centrifuged at 37,000 rpm in a TL-100 ultracentrifuge (Beckman, Mountain View, CA) for 20 min at 4^oC. The supernatant was precipitated by dropwise addition of an equal volume of saturated $(NH4)_2SO_4$. The precipitate was centrifuged at 16,000 x g for 15 min. Buffer C (50 mM HEPES pH7.5, 50 mM KOAc, 10 mM Mg_2OAc, 1 mM EDTA, 1 mM DTT, 10% glycerol, with protease and phosphatase inhibitors) was added to dissolve the pellet at a volume corresponding to $1/5^{th}$ of the original packed-cell volume. The lysate was then completely equilibrated into Buffer C by passage through a 0.5 ml Sephadex G-25 spin column. Final protein concentration was typically 15 mg/ml.

For pulldown reactions, 66 pmoles of GST fusion protein was pre-bound to 10 μl of glutathione-sepharose beads for 2 hr at 4°C. Nuclear lysate was diluted to 1 mg/ml in Buffer D (Buffer C + 0.1% NP-40 + 0.05% Triton X-100 + 0.2 mM PMSF) and centrifuged at 14,000 x g for 15 min. 100 μl of the supernatant was incubated at 4°C for 2 hr with 10 μl glutathione-sepharose beads to pre-clear the lysate of non-specific binding proteins. Cleared lysate was then incubated with 10 μl of GST-bound sepharose beads overnight at 4°C. Beads were washed three times in Buffer D before they were boiled in 2 x SDS-PAGE loading buffer without DTT. Eluate was adjusted to 100 mM DTT and re-boiled before it was subjected to 7.5% SDS-PAGE and Western analysis.

Bioinformatics

For RNA-seq analysis, we used EdgeR and an estimate of the biological coefficient of variation (BCV) to fit the data to a negative binomial model and estimate the significance of differentially expressed miRNAs (Robinson et al., 2010). Specifically, we used the raw number of reads as input for EdgeR, which first normalizes the libraries for any variation in sequencing depth/library size. We then fit the data to a negative binomial model using the function rnbinom and chose a nominal BCV value of 0.1 to calculate the dispersion. We next used the exactTest function (which parallels a Fisher's exact test for a negative binomial model) to calculate significance. MicroRNAs with an FDR adjusted p-value (q-value) < 0.05 were considered significant.

Motif analysis of pri-miRNA hairpins was performed using Probability Logo (Plogo) (O'Shea et al., 2013). Residue heights in a pLogo are closely proportional to the log(base10) odds of the significance of overrepresentation versus the significance of underrepresentation for that RNA base. These significance values are calculated using the binomial probability of base frequencies, with respect to a background data set (in this case the set of complete pre-miRNA sequences). The use of this log-odds approximation of the binomial probability for pLogo residue heights has the following attractive properties: (i) it is intuitive, as it closely represents the log odds of overrepresentation; (ii) it has a value of 0 (or very close to 0) when a residue is neither underrepresented nor overrepresented; (iii) if a base is substantially underrepresented or overrepresented, one probability will be very small and the other will be near 1.0; thus, being toward one tail or the other will hardly be affected at all by the weight of the other tail.

Sequences representing the Pfam WW domain family seed alignment were derived from the Protein family database (Finn et al., 2010). A multiple sequence alignment and phylogenetic tree were constructed with Clustal W2 and the Mobyle Portal programs Prodist and Neighbor (Neron et al., 2009).

To model predicted pre-miRNA structures, we extracted pre-miRNA sequences from miRbase. These were independently inputted into the folding programs mFold (Zuker, 2003) and RNAfold (Hofacker, 2003) using default settings. A consensus structure for each hairpin-loop was derived from the output from both programs.

SUPPLEMENTAL REFERENCES

Brodsky, A.S., Meyer, C.A., Swinburne, I.A., Hall, G., Keenan, B.J., Liu, X.S., Fox, E.A., and Silver, P.A. (2005). Genomic mapping of RNA polymerase II reveals sites of co-transcriptional regulation in human cells. Genome Biol *6*, R64.

Finn, R.D., Mistry, J., Tate, J., Coggill, P., Heger, A., Pollington, J.E., Gavin, O.L., Gunasekaran, P., Ceric, G., Forslund, K.*, et al.* (2010). The Pfam protein families database. Nucleic Acids Res *38*, D211-222.

Hofacker, I.L. (2003). Vienna RNA secondary structure server. Nucleic Acids Res *31*, 3429-3431.

Hoffman, S.J., Looker, D.L., Roehrich, J.M., Cozart, P.E., Durfee, S.L., Tedesco, J.L., and Stetler, G.L. (1990). Expression of fully functional tetrameric human hemoglobin in Escherichia coli. Proc Natl Acad Sci U S A *87*, 8521-8525.

Kim, M., Krogan, N.J., Vasiljeva, L., Rando, O.J., Nedea, E., Greenblatt, J.F., and Buratowski, S. (2004). The yeast Rat1 exonuclease promotes transcription termination by RNA polymerase II. Nature *432*, 517-522.

Neron, B., Menager, H., Maufrais, C., Joly, N., Maupetit, J., Letort, S., Carrere, S., Tuffery, P., and Letondal, C. (2009). Mobyle: a new full web bioinformatics framework. Bioinformatics *25*, 3005-3011.

O'Shea, J.P., Chou, M.F., Quader, S.A., Ryan, J.K., Church, G.M., and Schwartz, D. (2013). pLogo: a probabilistic approach to visualizing sequence motifs. Nat Methods *10*, 1211-1212.

Robinson, M.D., McCarthy, D.J., and Smyth, G.K. (2010). edgeR: a Bioconductor package for differential expression analysis of digital gene expression data. Bioinformatics *26*, 139-140.

Sambrook, J., and Russell, D. (2001). Molecular Cloning A Laboratory Manual, Vol 2, Third edn (New York: Cold Spring Harbor Press).

Schroder, S., Herker, E., Itzen, F., He, D., Thomas, S., Gilchrist, D.A., Kaehlcke, K., Cho, S., Pollard, K.S., Capra, J.A.*, et al.* (2013). Acetylation of RNA polymerase II regulates growth-factor-induced gene transcription in mammalian cells. Mol Cell *52*, 314-324.

Wright, K.J., Marr, M.T., 2nd, and Tjian, R. (2006). TAF4 nucleates a core subcomplex of TFIID and mediates activated transcription from a TATA-less promoter. Proc Natl Acad Sci U S A *103*, 12347-12352.

Zuker, M. (2003). Mfold web server for nucleic acid folding and hybridization prediction. Nucleic Acids Res *31*, 3406-3415.